

Shear rate dependence of the pāhoehoe-to-‘a‘ā transition: Analog experiments

S. Adam Soule Department of Geology and Geophysics, Woods Hole Oceanographic Institution, Woods Hole, Massachusetts 02543, USA

Katharine V. Cashman Department of Geological Sciences, University of Oregon, Eugene, Oregon 97403-1272, USA

ABSTRACT

Hawaiian lava flows typically erupt as pāhoehoe and transform to ‘a‘ā as they travel away from eruptive vents, although the exact conditions that govern this transformation are not well constrained. Here we describe a set of laboratory experiments that use corn syrup and ellipsoidal rice grains as an analog to lava with crystals to examine the dependence of the transition on shear rate and particle concentration. At a particle volume fraction of 0.3, increasing the shear rate produces a sequence of deformation regimes defined by increasing amounts of shear localization. The same regimes may be traversed at constant shear rate by varying the particle concentration. At high shear rates, the onset of nonlaminar deformation corresponds to the percolation threshold, thus providing a link between suspension microstructure and deformation behavior. Together these results highlight the combined importance of shear rate and crystallinity in determining the flow behavior of basaltic lava.

Keywords: basaltic lava flows, rheology, shear localization, flow dynamics.

INTRODUCTION

Basaltic lava flows are classified as pāhoehoe or ‘a‘ā by their surface morphology, i.e., smooth and continuous for pāhoehoe and rough and fragmental for ‘a‘ā (Fig. 1; e.g., Dutton, 1884; Dana, 1849; Macdonald, 1953). As originally defined, the terms pāhoehoe and ‘a‘ā described only the solidified flow surface. However, observations of active flows have led to the association of these two morphologic types with specific physical properties of the lava (Cashman et al., 1999), eruption conditions (Rowland and Walker, 1990), and styles of flow advance (Kilburn, 1996). These associations allow interpretation of older flows (e.g., Soule et al., 2004) and prediction of active flow advance (e.g., Pinkerton and Wilson, 1994).

Peterson and Tilling (1980) first described

the pāhoehoe-to-‘a‘ā transition as an inverse relationship between the apparent viscosity (η_a) of the lava and the shear rate ($\dot{\gamma}$) applied to the flow. In Bingham fluids η_a is a function of both the strain rate and the fluid yield strength (Kilburn, 1981), which in turn is controlled by the crystal content of the lava (Cashman et al., 1999). Within a limited range of (constant) apparent viscosity, lava may advance as either pāhoehoe or ‘a‘ā, depending on the local strain rate. Also important in the transition is the failure behavior of the solid flow crust, which changes from intermittent to persistent as the flow-emplacment style changes from pāhoehoe to ‘a‘ā (Kilburn, 1981, 2004).

The relationship between the failure behavior of surface crusts and the physical properties of the fluid flow interior is poorly under-

stood, in part because of our limited understanding of the nature of crystal-crystal interactions during flow. In particular, rheological experiments on nondilute suspensions demonstrate the potential importance of flow-induced material instabilities such as phase separation, shear banding, and constant-force chains that result in nonlinear strain in response to a constant applied stress (e.g., Goddard, 2003). Here we investigate these phenomena in analog laboratory experiments designed to simulate the behavior of flowing crystal-bearing lava. We observe marked transitions in deformation style caused by different scales of shear localization, map the onset of those deformation styles as a function of shear rate and particle concentration, and discuss possible analogs for each deformation style in natural lava flows.

EXPERIMENTAL SETUP

In our experiments we used corn syrup diluted with water to achieve a viscosity of ~50–100 Pa·s, similar to crystal-free basaltic liquid (Hoover et al., 2001). To the viscous fluid we added rice grains to produce suspensions with particle concentrations (ϕ) of 0.15–0.4. The near neutral buoyancy of the rice grains ($\rho = 1470 \text{ kg/m}^3$) relative to the corn syrup ($\rho = 1440 \text{ kg/m}^3$) allows the particles to stay in suspension through the duration of an experimental run. Although ellipsoidal rice grains are not a perfect analog for the combination of tabular plagioclase and near-equant pyroxene microphenocrysts common



Figure 1. Left: pāhoehoe lavas, with smooth, ropy crusts, are emplaced as lobes or toes that advance discontinuously. Width of view is ~3 m. Right: ‘a‘ā lavas, with rough, fragmental crusts, are emplaced as sheets or channels that advance continuously. Flow front is ~2 m in height. Photos courtesy of Hawaiian Volcanoes Observatory, U.S. Geological Survey.

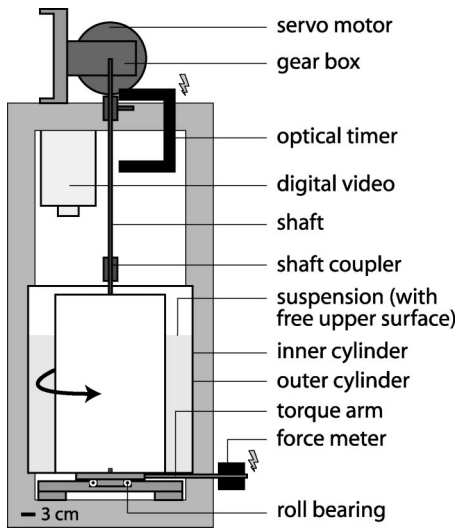


Figure 2. Vertical cross section of experimental apparatus. Experiments were run with outer cylinder fixed while one-half horsepower DC motor rotated inner cylinder. Rotation rate was measured with optically triggered timing device. Each experiment involved suspension of constant particle concentration (ϕ) with stepwise increases in rotation rate from ~ 0.1 to 35 rpm. Force meter attached to outer cylinder measured torque transmitted to suspension. Rheometer mounted in roll bearing attached to outer cylinder reduced frictional forces that could decrease measured torque. Experiments were run with free upper surface that was observed from above and recorded with digital video camera. Lightning-bolt symbols indicate sensors that detect data to be recorded with data logger during experimental runs.

to Hawaiian basalt (Cashman et al., 1999), the regular shape and aspect ratio ($\sim 3:1$) of the rice grain permit us to relate particle concentration directly to yield strength through percolation theory models (Saar et al., 2001; Saar and Manga, 2002), which have also been applied to crystal assemblages in basaltic lava (Philpotts and Carroll, 1996; Hoover et al., 2001).

Experiments were performed in a coaxial cylinder (Couette) rheometer (Fig. 2) with a coating of rice on interior surfaces providing surface roughness of a length scale similar to that of the fluid suspension (e.g., Nguyen and Boger, 1992). Paths of individual particles were both observed in real time and recorded with a digital video camera, with observations of the suspension microstructure at its free upper surface aided by coloring individual rice grains. We avoided recording transient phenomena by making observations only after the fluid had deformed at a constant rotation rate for ~ 30 s. The ratio of outer to inner cylinder radii (r_{oi}) and the ratio of particle size to gap width between the cylinders (e.g., Nguyen and Boger, 1992) are important for experiment reproducibility. We used a gap width of 10 cm

(an order of magnitude larger than individual rice grains) and $r_{oi} = 1.5$ and 2. The larger r_{oi} provided sufficient surface area to describe particle interactions over the full range of rotation rates and particle concentrations, but resulted in a small variability in shear rate across the gap. Rotation rate can be converted directly to shear rate if r_{oi} is between 1.2 and 1.5 (Krieger and Dougherty, 1959). A second set of experiments with $\phi = 0.30$ and a radius ratio of 1.5 permitted determination of applied shear rate with the empirically derived Krieger-Maron equation (Krieger and Dougherty, 1959):

$$\dot{\gamma} = \frac{4\pi N}{1 - \frac{1}{S^2}} \left[1 + K_1 \left(\frac{1}{n''} - 1 \right) + K_2 \left[\left(\frac{1}{n''} - 1 \right) + \frac{\partial[(1/n'') - 1]}{\partial(\log M)} \right] \right], \quad (1)$$

where N is rotational speed, M is torque, n'' is the slope of a logarithmic plot of M vs. N , and S is the ratio of the outer to inner cylinder radius. K_1 and K_2 are constants of the instrument described by

$$K_1 = \frac{S^2 - 1}{2S^2} \left(1 + \frac{2}{3} \ln S \right) \quad \text{and} \quad (2)$$

$$K_2 = \frac{S^2 - 1}{6S^2} (\ln S). \quad (3)$$

Rotation rates of 0.35–12.50 rpm generate shear rates that range from 0.1 to 3.6 s^{-1} .

SUSPENSION DEFORMATION

Four deformational regimes can be defined based on distinct changes in particle interaction style (Fig. 3). We first describe deformational regimes and the transitions caused by changing shear rate at a single particle concentration ($\phi = 0.3$). At the lowest rotation rates ($\dot{\gamma} < 0.24 s^{-1}$) deformation is laminar, with particles moving along parallel flow paths at velocities that increase as a function of distance from the inner cylinder (Fig. 3A). In laminar flow, grains may rotate freely (Jeffrey orbits; e.g., Larson, 1999), but particle paths rarely cross. At ($\dot{\gamma} > 0.24 s^{-1}$), particles form clumps of 10 or more that rotate opposite to the rotation direction of the inner cylinder while gradually migrating toward the outer cylinder (Fig. 3B). Clump rotation thus produces transverse particle paths and particle-free shadows behind rotating clumps. Clump formation is near the outer cylinder at low rotation rates and moves inward as rotation rate increases. Once formed, clumps grow by adhesion of additional free particles. Typically

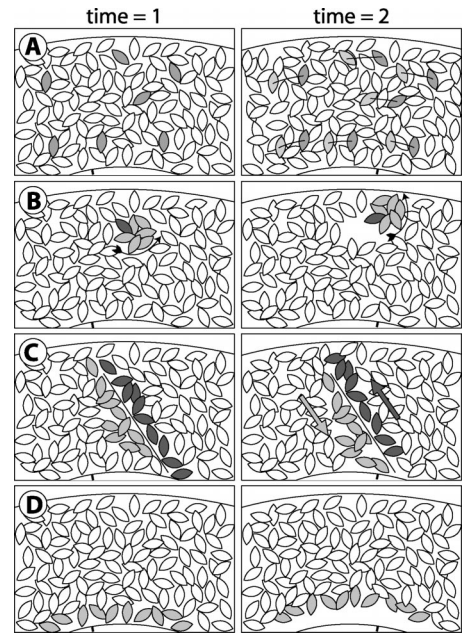
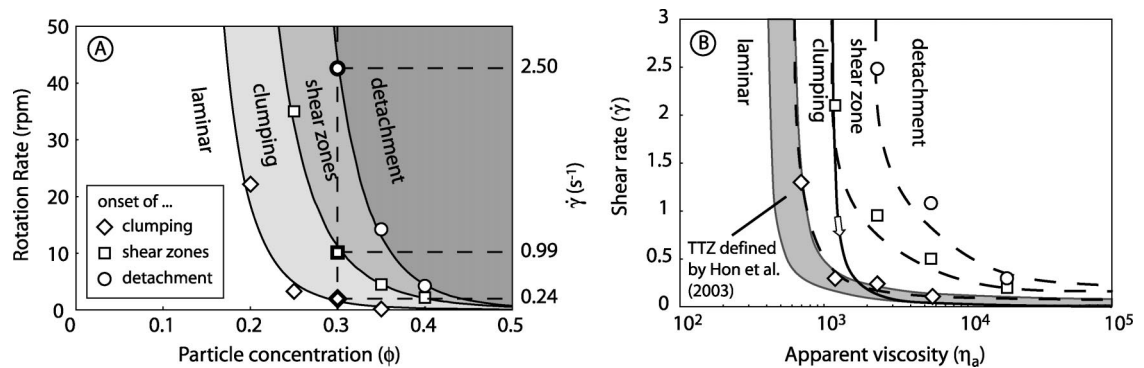


Figure 3. Deformation mechanisms observed from above area between cylinders during experiments. **A:** laminar flow. **B:** clumping. **C:** shear-zone formation. **D:** detachment. Filled grains highlight deformation styles. In all diagrams, direction of rotation of inner cylinder, located at base of each figure, is clockwise; outer cylinder remains fixed.

clumps persist for ~ 3 s at low rotation rates and < 1 s at higher rates, at which point the stress on the clump exceeds the viscous forces holding particles together and the clump disperses.

The deformation style changes at $\dot{\gamma} \geq 1 s^{-1}$, with through-going transverse shear zones forming as clumps accumulate near the outer cylinder, eventually causing the suspension to lock up (e.g., Cheng and Richmond, 1978; Fig. 3C). With continued deformation, shear zones stretch and degrade until new shear zones replace them. In detail, shear zones appear to form when closely packed particles separate (dilate) to move past each other. This shear dilatancy (e.g., Smith, 2000) is accompanied by an increase in normal stress, which may explain the arching of the suspension surface observed in experiments at high shear rates (as commonly observed in crystal-rich 'a'ā flows at Mount Etna). The highest shear rates ($\dot{\gamma} \geq 2.5 s^{-1}$) cause the suspension to detach completely from the inner cylinder wall, creating a gap that is traversed by thin strands of corn syrup. The detachment increases in both depth (from the upper suspension surface) and width (between the suspension and inner cylinder) with increasing rotation rate, reaching maximum depths of ~ 1 cm and widths of ~ 0.5 cm for the shear-rate limit of our apparatus ($\dot{\gamma} \leq 6 s^{-1}$). Detachment is not the result of fluid failure, as no detachment

Figure 4. A: Onset of clumping (diamond), shear-zone formation (square), and detachment (circle) shown as function of particle concentration (ϕ) and rotation rate (rpm). Corresponding shear rates are constrained by experiments conducted at $\phi = 0.3$ (bold symbols; dashed line). TTZ—transition threshold zone. B: Our data are compared to field estimates of pāhoehoe-to-‘a‘ā transition in $\eta_a - \dot{\gamma}$ space (after Hon et al., 2003). Our regime boundaries (dashed lines), which are well constrained at low ϕ and $\dot{\gamma}$, confirm placement and shape of transition zone between pāhoehoe and ‘a‘ā suggested by Hon et al. (2003). Asymptotic approach of regime boundaries to apparent viscosity axis at low $\dot{\gamma}$ indicates that laminar deformation may occur even at high ϕ . Apparent viscosity curve for typical Mauna Loa lava (solid line) shows how lava subjected to decreasing shear rate might pass through pāhoehoe-to-‘a‘ā transition.



occurred in tests on pure corn syrup, but instead appears to result from cavitation at the fluid-particle interface due to the steep gradient in shear. Cavitation has been documented in silicic lavas where fluid viscosities are large (Smith et al., 2001); our results suggest that similar processes may occur in particle-rich suspensions of low-viscosity liquids.

A summary of experimental results (Fig. 4A) shows that the same deformation regimes may be traversed in the same order (from laminar flow to detachment) at a constant shear rate by increasing the particle concentration. Laminar deformation is observed for all ϕ at the lowest shear rates and persists to the limits of the apparatus ($\dot{\gamma} \sim 6 \text{ s}^{-1}$) for the lowest ϕ (0.15). At $0.2 < \phi < 0.3$, clumps appear at $1 < \dot{\gamma} < 2 \text{ s}^{-1}$, with the number of particles in each clump approximately proportional to ϕ . Detachment requires $\phi \geq \sim 0.30$ and moderate to high rates of shear when $\phi < 0.4$. Limiting values of $\phi < \sim 0.2$ for laminar flow behavior at all shear rates can be explained with reference to percolation models (Saar et al., 2001; Saar and Manga, 2002) that predict the onset of touching networks of randomly oriented particles at $\phi \sim 0.20$ for particle aspect ratios appropriate for rice grains, a criterion also suggested to reflect the onset of yield strength (Kerr and Lister, 1991). This correlation suggests that the percolation threshold may be a good predictor for the onset of material instabilities and shear localization.

DISCUSSION

The deformation mechanisms—clumping, shear-zone formation, and detachment—observed in our experiments reflect material instabilities in the particle-fluid suspensions that localize applied shear stresses. Moreover, the observation that deformation regime boundaries may be crossed by changing either particle concentration (apparent viscosity) or shear rate is consistent with proposed models

for the pāhoehoe-to-‘a‘ā transition. An important difference between our experiments and basaltic lava flows, however, is the role of cooling. As our experiments are isothermal, transitions between deformation regimes are completely reversible and are thus not maintained once deformation ceases. In contrast, rapid quenching of basaltic lava flow surfaces during deformation preserves the shear-induced surface morphology. Thus if the deformation regimes shown in Figure 4A are applicable to Hawaiian lava flows, we might expect flow surface morphology to reflect down-flow changes in lava crystallinity (from cooling) and flow rate. In Hawai‘i, near-vent pāhoehoe commonly gives way to spiny, then clinkery lava fragments (e.g., Macdonald, 1953). Spiny surface regions first form as clots of cooler crust in regions of high shear (typically at the flow margins; Wentworth and Macdonald, 1953; Peterson and Tilling, 1980; Kilburn, 1990), analogous to our clumping regime. Further shear localization creates distinct spiny (and quenched) fragments that rotate across the flow surface toward the center of the channel, away from regions of highest shear, eventually covering the entire flow. Further cooling and crystallization along margins of mature ‘a‘ā channels may result in the formation of detachment surfaces between the moving fluid and the channel wall (e.g., Wolfe et al., 1988), analogous to our most extreme example of shear localization. Detachment behavior may mark the onset of brittle failure, thus relating to the fracture criterion described by Kilburn (2004). Together these stages of progressive shear localization give ‘a‘ā its characteristic rough and fragmental surface.

We extend this analogy by noting that regime boundaries in Figure 4A have the same general form as the transition boundary on a plot of effective viscosity vs. shear rate (Peterson and Tilling, 1980; Kilburn, 1981, 1990; Hon et al., 2003), although our regime bound-

aries are defined by particle concentration (ϕ) rather than apparent viscosity (η_a). Moreover, the range of shear rate ($0.1 \leq \dot{\gamma} \leq 3.6 \text{ s}^{-1}$) and particle concentration ($0.15 \leq \phi \leq 0.4$) that we investigated is similar to that reported for Hawaiian lava flows ($0.1 \leq \dot{\gamma} \leq 5 \text{ s}^{-1}$; $\phi \leq 0.5$; Lipman and Banks, 1987; Cashman et al., 1999; Katz and Cashman, 2003; Soule et al., 2004). Furthermore, these studies suggest that smooth pāhoehoe flow surfaces form only for $\phi < 0.2$, consistent with the experimentally defined limit to laminar flow behavior. Direct comparison of our data with the semi-quantitative flow regime diagram of Hon et al. (2003) requires conversion of ϕ to η_a . An exact relationship between η_a and ϕ remains elusive as it depends on particle size, particle shape, and shear rate (Gay et al., 1969; Wildemuth and Williams, 1984; Kerr and Lister, 1991; Pinkerton and Stevenson, 1992; Zhou et al., 1995). A general description of the effect of particle concentration on the viscosity of a low-concentration suspension, the Einstein-Roscoe equation (1953), was extended by Marsh (1981) to higher concentrations ($\phi > 0.2$),

$$\eta_{\text{susp}} = \eta_{\text{liquid}}(1 - \phi/\phi_m)^{-2.5}, \quad (4)$$

where ϕ_m is the maximum packing fraction. Pinkerton and Stevenson (1992) found this description of suspension viscosity (η_{susp}) to be an adequate approximation for η_a , but warned that predicted viscosities may differ by a factor of 3 or more from measured viscosities. The theoretical value of ϕ_m for uniform spheres is $\phi = 0.74$, but values are expected to decrease dramatically with increasing particle aspect ratio. We choose a conservative ϕ_m of 0.55 for our particles (cf. Pinkerton and Stevenson, 1992) and note that further experimental work is necessary to refine our estimate of ϕ_m .

Using this approximation we can compare our data directly to the semiquantitative

portrayal of the pāhoehoe-to-‘a‘ā transition boundary presented in Hon et al. (2003), as defined by field measurements on Hawaiian lava flows (Fig. 4B). Our boundary for the onset of clumping behavior coincides with Hon et al.’s (2003) placement of the transition threshold zone (as defined by Peterson and Tilling, 1980), the boundary between pāhoehoe and ‘a‘ā flow regimes. Moreover, our data, which are well constrained at low shear rates, support Hon et al.’s (2003) interpretation of an asymptotic approach of the deformation boundaries to the apparent viscosity axis, which predicts that laminar flow may occur at high ϕ (η_a) when the strain rate is sufficiently low. However, as the flow regime boundaries are dependent primarily on ϕ (η_a) and independent of $\dot{\gamma}$ except at low shear rates (Fig. 4B), large observed down-flow changes in crystallinity are likely to exert the primary control on emplacement style (and surface morphology) of Hawaiian lava flows (e.g., Cashman et al., 1999; Hon et al., 2003; Soule et al., 2004).

Our data help to explain recent observations of ‘a‘ā flow fronts transforming to pāhoehoe styles of flow advance (Calvari and Pinkerton, 1998; Hon et al., 2003). Figure 4B shows that such reversibility is possible for lava with intermediate crystal contents and shear rates that drop below the bounding curve for clumping behavior. Pāhoehoe breakouts have been observed from ‘a‘ā flow fronts at Mount Etna that stalled and inflated on near-horizontal slopes (Calvari and Pinkerton, 1998). Alternatively, upstream lava tube formation described by Hon et al. (2003) may permit near-liquidus (crystal poor) Hawaiian lava to reach flow fronts without cooling sufficiently to reach the critical crystallinity for ‘a‘ā formation, thus explaining observed reversibility in recent lava flows from Hawai‘i (Hon et al., 2003). In summary, we have identified flow deformation regimes in viscous suspensions that provide new insight into the pāhoehoe-to-‘a‘ā transition mechanisms in basaltic lava and place constraints on the range of particle concentration (crystallinity) and strain rates over which these mechanisms operate.

ACKNOWLEDGMENTS

This work was supported by National Science Foundation grant EAR-0207919 to Cashman. We thank M. Manga for useful discussions of the results of this research and D. Senkovitch and K. Johnson for assistance in the development of the experimental apparatus. The manuscript was greatly improved by reviews from S. Calvari, C. Kilburn, and S. Rowland.

REFERENCES CITED

Calvari, S., and Pinkerton, H., 1998, Formation of lava tubes and extensive flow field during the 1991–93 eruption of Mount Etna: *Journal of Geophysical Research*, v. 103, p. 27,291–27,302.

- Cashman, K.V., Thornber, C., and Kauahikaua, J.P., 1999, Cooling and crystallization of lava in open channels, and the transition of pahoehoe lava to ‘a‘ā: *Bulletin of Volcanology*, v. 61, p. 306–323.
- Cheng, D.-H., and Richmond, R., 1978, Some observations on the rheological behaviour of dense suspensions: *Rheologica Acta*, v. 17, p. 446–453.
- Dana, J.D., 1849, *Geology: United States Exploring Expedition*: New York, George P. Putnam, 756 p.
- Dutton, C.E., 1884, Hawaiian volcanoes: U.S. Geological Survey Annual Report, no. 4, p. 75–219.
- Gay, E.C., Nelson, P.A., and Armstrong, W.P., 1969, Flow properties of suspensions with high solids concentrations: *American Institute of Chemical Engineering Journal*, v. 15, p. 815–822.
- Goddard, J.D., 2003, Material instability in complex fluids: *Annual Review of Fluid Mechanics*, v. 35, p. 113–133.
- Hon, K.A., Gansecki, C., and Kauahikaua, J., 2003, The transition from ‘a‘ā to pāhoehoe crust on flows emplaced during the Pu‘u ‘O‘o-Kupaianaha eruption, in Heliker, C.A., et al., eds., *The Pu‘u ‘O‘o-Kupaianaha eruption of Kilauea volcano, Hawai‘i: The first 20 years*: U.S. Geological Survey Professional Paper 1676, p. 89–104.
- Hoover, S.R., Cashman, K.V., and Manga, M., 2001, The yield strength of subliquidus basalts: Experimental results: *Journal of Volcanology and Geothermal Research*, v. 107, p. 1–18.
- Katz, M.G., and Cashman, K.V., 2003, Hawaiian lava flows in the third dimension: Identification and interpretation of pāhoehoe and ‘a‘ā distribution in the KP-1 and SOH-4 cores: *Geochemistry, Geophysics, Geosystems* (G³), v. 4, 8705, doi: 10.1029/2001GC000209.
- Kerr, R.C., and Lister, J.R., 1991, The effects of shape on crystal settling and on the rheology of magmas: *Journal of Geology*, v. 99, p. 457–467.
- Kilburn, C.R., 1981, Pāhoehoe and ‘a‘ā lavas: A discussion and continuation of the model of Peterson and Tilling: *Journal of Volcanology and Geothermal Research*, v. 11, p. 373–382.
- Kilburn, C.R., 1990, Surfaces of aa flow-fields on Mount Etna, Sicily; morphology, rheology, crystallization and scaling phenomena, in Fink, J.H., ed., *Lava flows and domes; emplacement mechanisms and hazard implications*: Berlin, Springer Verlag, p. 129–156.
- Kilburn, C.R.J., 1996, Patterns and predictability in the emplacement of subaerial lava flows and flow fields, in Scarpa, R., and Tilling, R.I., eds., *Monitoring and mitigation of volcano hazards*: Berlin, Springer-Verlag, p. 491–537.
- Kilburn, C.R.J., 2004, Fracturing as a quantitative indicator of lava flow dynamics: *Journal of Volcanology and Geothermal Research*, v. 132, p. 209–224.
- Krieger, I., and Dougherty, T., 1959, A mechanism for non-Newtonian flow in suspensions of rigid spheres: *Society of Rheology Transactions*, v. 3, p. 137–152.
- Larson, R., 1999, *The structure and rheology of complex fluids*: New York, Oxford University Press, 663 p.
- Lipman, P., and Banks, N., 1987, ‘A‘ā flow dynamics, Mauna Loa 1984, in Decker, R.W., et al., eds., *Volcanism in Hawaii, Volume 2*: U.S. Geological Survey Professional Paper 1350, p. 1527–1567.
- Macdonald, G., 1953, Pāhoehoe, ‘a‘ā, and block lava: *American Journal of Science*, v. 251, p. 169–191.
- Marsh, B.D., 1981, On the crystallinity, probability of occurrence, and rheology of lava and magma: *Contributions to Mineralogy and Petrology*, v. 78, p. 85–98.
- Nguyen, Q., and Boger, D., 1992, Measuring the flow properties of yield stress fluids: *Annual Review of Fluid Mechanics*, v. 24, p. 47–88.
- Peterson, D.W., and Tilling, R.I., 1980, Transition of basaltic lava from pāhoehoe to ‘a‘ā, Kilauea volcano Hawaii: Field observations and key factors: *Journal of Volcanology and Geothermal Research*, v. 7, p. 271–293.
- Philpotts, A.R., and Carroll, M., 1996, Physical properties of partly melted tholeiitic basalt: *Geology*, v. 24, p. 1029–1032.
- Pinkerton, H., and Stevenson, R.J., 1992, Methods of determining the rheological properties of magmas at sub-liquidus temperatures: *Journal of Volcanology and Geothermal Research*, v. 53, p. 47–66.
- Pinkerton, H., and Wilson, L., 1994, Factors controlling the lengths of channel-fed lava flows: *Bulletin of Volcanology*, v. 56, p. 108–120.
- Roscoe, R., 1953, Suspensions, in Hermans, J.J., ed., *Flow properties of disperse systems*: Amsterdam, North Holland, p. 1–38.
- Rowland, S.K., and Walker, G.P., 1990, Pāhoehoe and ‘a‘ā in Hawaii: Volumetric flow rate controls the lava structure: *Bulletin of Volcanology*, v. 52, p. 615–628.
- Saar, M.O., Manga, M., Cashman, K.V., and Fermou, S., 2001, Numerical models of the onset of yield strength in crystal-melt suspensions: *Earth and Planetary Science Letters*, v. 187, p. 367–379.
- Saar, M.O., and Manga, M., 2002, Continuum percolation for randomly oriented soft-core prisms: *Physical Review E*, v. 65, p. 1–6.
- Smith, J., 2000, Textural evidence for dilatant (shear thickening) rheology of magma at high crystal concentrations: *Journal of Volcanology and Geothermal Research*, v. 99, p. 1–7.
- Smith, J., Miyake, Y., and Oikawa, T., 2001, Interpretation of porosity in dacite lava domes as ductile-brittle failure textures: *Journal of Volcanology and Geothermal Research*, v. 112, p. 25–35.
- Soule, S.A., Cashman, K.V., and Kauahikaua, J.P., 2004, Examining flow emplacement through the surface morphology of three rapidly emplaced, solidified lava flows, Kilauea Volcano, Hawaii: *Bulletin of Volcanology*, v. 66, p. 1–14.
- Wentworth, C.K., and Macdonald, G.A., 1953, Structures and forms of basaltic rocks in Hawaii: *U.S. Geological Survey Bulletin*, v. 994, 98 p.
- Wildemuth, C.R., and Williams, M.C., 1984, Viscosity of suspensions modeled with a shear-dependent maximum packing fraction: *Rheologica Acta*, v. 23, p. 627–635.
- Wolfe, E.W., Neal, C.A., Banks, N.G., and Duggan, T.J., 1988, Geologic observations and chronology of eruptive events, in Wolfe, E.W., ed., *The Puu Oo eruption of Kilauea volcano, Hawaii: Episodes 1 through 20, January 3, 1983, through June 8, 1984*: U.S. Geological Survey Professional Paper 1463, p. 1–98.
- Zhou, J.Z.Q., Fang, T., Luo, G., and Uhlherr, P.H.T., 1995, Yield stress and maximum packing fraction of concentrated suspensions: *Rheologica Acta*, v. 34, p. 544–561.

Manuscript received 15 October 2004

Revised manuscript received 24 January 2005

Manuscript accepted 26 January 2005

Printed in USA